A novel working fluid for Organic Rankine Cycles (ORC)

A S PANESAR, M R HEIKAL, M MARENGO and R E MORGAN
School of Computing, Engineering and Mathematics, University of Brighton, UK

ABSTRACT

The use of ORCs on long-haul Heavy Duty Diesel Engines (HDDE) is a possible way to improve the specific fuel consumption. One of the key considerations in the research and development efforts for ORCs is to investigate and identify technical paths that may improve the practicality of such a heat to power conversion concept. For this, simple solutions are vital for a timely deployment of the technology to meet the anticipated CO_2 regulations.

To provide a potential solution, this paper presents the simulation results of a novel organic working fluid (using Aspen HYSYS) which has been especially formulated for the HDDE sector. Due to the unique heat transfer and expansion characteristics, the primary advantage of the novel working fluid included an equivalent performance to ethanol despite a 20% reduction in the total heat transfer area and a 20% reduction in the size of the expansion machine. The secondary advantages over ethanol included a higher molecular weight (Δ 20 g/mol) and the requirement of a lower maximum system pressure (Δ 15 bar). Additionally, the novel fluid is expected to offer low global warming potential (< 20) and a high thermal stability (≈ 360°C).

1 INTRODUCTION

In a typical internal combustion engine about 1/3rd of the total fuel energy is wasted in the form of exhaust gas heat. Converting this waste heat into usable mechanical or electrical power is seen as a key area in the development of low carbon powertrains [1, 2]. This is an ongoing area of intensified research, where numerous methods have been demonstrated. These methods include, but are not limited to, turbocompounding (mechanical, electrical), thermoelectric generators and fluid bottoming cycles [3-6].

Amongst the fluid bottoming cycle options, ORCs are shown to be better adapted to an output capacity of 5-25 kW and heat source quality < 400°C [7, 8]. ORCs are in fact being adopted as a premier technology for long-haul HDDEs when considering conversion efficiencies, technology readiness level, impending CO_2 legislations, absolute fuel consumption, base vehicle cost, space availability and weight penalty. Key ORC components like heat exchangers (HEX) and expansion machines (piston expanders, radial turbines) are becoming more viable due to a series of recent technological advancements and synergies with the current automotive components

[9-11]. The current market niche for ORCs is dependent on simplicity and affordability, with initial technology deployment on commercial vehicles expected in the 2020-2022 timeframe.

The two widely proposed fluids for HDDE applications are R245fa and ethanol. These fluids are not without their distinctive challenges. R245fa has a relatively high global warming potential (1030, relative to CO_2 for an integration time horizon of 100 years) and an unfavourable thermal stability temperature limit (≈ 260°C), while ethanol has a relatively lower molecular weight (46 g/mol) and requires a larger expansion machine size [12, 13]. Although, the molecular make-up of organic fluids fundamentally precludes the possibility of an ideal fluid, ethanol is generally considered to offer a suitable trade-off [14].

2 BASELINE ETHANOL ORGANIC RANKINE CYCLE

This section presents the simulation results for an ethanol ORC with an Internal Heat Exchanger (IHE) to act as a reference for comparison. The simulations were conducted in an advanced chemical process modelling tool, Aspen HYSYS [15]. Only exhaust heat recovery, downstream of the aftertreatment devices, was considered at mid-speed mid-load (B50) from a 12.8 litre engine. This engine also utilised Exhaust Gas Recirculation (EGR). However, due to the lower EGR rates (< 15%) and further expected improvements in selective catalytic reduction technology, it is likely that by 2020-2022, HDDEs would offer exhaust as the only source of high quality and high quantity waste heat [16, 17]. Excluding EGR will also reduce the diesel particulate filter regeneration frequency. Although, regenerations can raise exhaust temperature above 600°C, ORC operation has to be stopped to avoid thermal degradation of the fluid.

Table 1 Assumptions and boundary conditions used in ORC simulations

Base engine performance (B50) ▪ BSFC = 195 g/kWh ▪ Crankshaft power = 158 kW *Non-insulated exhaust pipe* ▪ $T_{post-turbocharger\ turbine} = 420°C$ ▪ $T_{post-SCR} = 410°C$ ▪ $c_{p\ exhaust} = 1.14$ kJ/kg°C ▪ $m_{exhaust} = 0.22$ kg/s *Air condenser (counter-current)* ▪ $T_{condensing\ organic\ fluid} = 105°C$ ▪ $T_{sub-cooling} = 5°C$ ▪ $\Delta P_{organic\ fluid} = 0.2$ bar ▪ $T_{cooling\ air\ inlet} = 50°C$ ▪ $T_{cooling\ air\ outlet} = 65°C$	*Heat exchanger (counter-current)* ▪ $T_{HEX\ inlet} = 400°C$ ▪ $T_{max\ organic\ fluid} = 300°C$ ▪ $\Delta P_{exhaust} = 0.1$ bar ▪ $\Delta P_{organic\ fluid} = 0.5$ bar ▪ $T_{pinch\ point\ HEX} = 15°C$ *Internal heat exchanger (counter-current)* ▪ $T_{pinch\ point\ IHE} = 15°C$ ▪ $\Delta P_{IHE} = 0.2$ bar (each side) *Expansion machine and pump* ▪ $\eta_{expansion} = 70\%$ ▪ $\eta_{pump} = 60\%$ ▪ $\eta_{transmission} = 93\%$

Table 1 summarises the ORC modelling assumptions and boundary conditions used corresponding to realistic temperatures (exhaust, cooling air), component efficiencies

(η), performances ($T_{pinch\ point}$) and pressure losses (ΔP). To limit the fan power requirement and the total engine cooling-module size, a high-temperature direct air-cooled ORC condenser was used and positioned after the engine radiator. Furthermore, the maximum temperature of ethanol was restricted to 300°C. This is since the maximum fluid temperature is experienced at the boundary layer. This film region is typically 25°C higher than the bulk fluid temperature [18]. With ethanol molecule thermally decomposing at ≈350°C, the 300°C limit offered a 25°C safety margin [19].

Fig. 1a shows the layout of the simulated ORC. The purpose of using an IHE was to internally utilise the considerable exergy exiting the expansion machine, and hence avoid the potential loss in the condenser. The IHE increases the cycle thermal efficiency, decreases the heat recovery efficiency and has no impact on the net power. The improvement in the thermal efficiency results in reduced load on the condenser. The exclusion of low temperature exhaust heat recovery avoids corrosion and fouling in the HEX. Since the pressure difference across the expansion remains nearly equal, the specific work is unchanged.

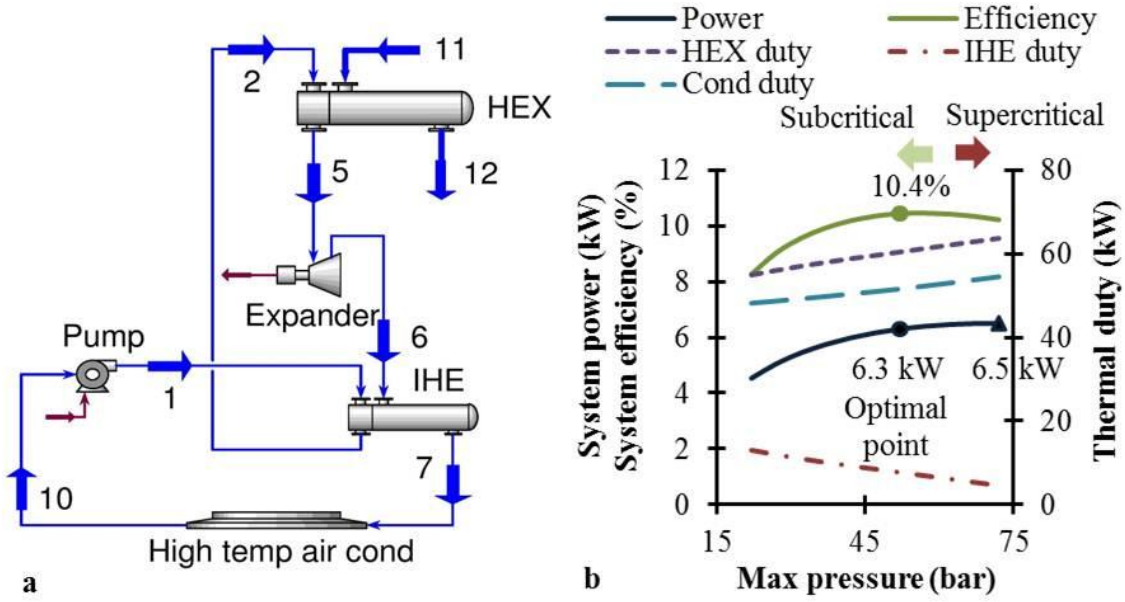

Figure 1 (a) ORC setup with IHE used in simulations (b) Optimisation results for ethanol

The ORC system power was calculated according to Equation 1.

$$ORC_{system} = \eta_{transmission}(W_{expansion} - W_{pump}) - W_{control+machine\ cooling} - W_{backpressure+\ fan\ power} \ldots (1)$$

Where, $W_{backpressure+\ fan\ power} = 0.003 Q_{HEX}^{1.5} \ldots (2)$

Equation 1 includes a fixed 0.5 kW requirement for controls and expansion machine cooling. An earlier correlation (Equation 2) was used to calculate the combined effect of increased fan power requirement and the power loss due to backpressure depending on the duty of the HEX. As an approximation, for heat recovery at B50, this corresponded to ≈1% of the engine crankshaft power consumption.

Fig. 1b shows the pressure optimisation results for the ethanol ORC with an IHE. A maximum cycle pressure of 52 bar ($0.85\,P_{critical}$) was considered optimal since the rate of system power improvement was rather inadequate with higher pressures. For organic fluids with boiling points between 40-80°C, slightly subcritical evaporator pressures usually offer optimal results under high source temperature (400°C) and high source-to-sink temperature differential (Δ 350°C), as was in the present case [20]. This pressure value also corresponded to the peak system thermal efficiency of 10.4%.

Table 2 summarises the optimal system performance and property values for ethanol. The system required a high expansion Volume Flow Ratio (VFR 16:1) and Pressure Ratio (PR 16.3:1), making it better suited to piston expanders. The requirement of a large expansion machine size with ethanol is fundamentally related to a higher $T_{boil\ low\ pressure}$ / $T_{boil\ high\ pressure}$ value.

Table 2 Performance and property values for ethanol and E40

	Ethanol	E40
$P_{max}\ bar$	52	37
$P_{min}\ bar$	2.8	2.2
$T_{max}\ °C$	300	300
$T_{min}\ °C$	100	94
$T_{condensation}\ °C$ (avg. for E40)	105	103
$T_{evaporation}\ °C$ (avg. for E40)	230	234
$m_{fluid}\ kg/s$	0.06	0.08
$UA_{HEX} W/°C$	1791	1433
$UA_{IHE} W/°C$	275	220
$UA_{Cond} W/°C$	1027	822
$m_{air}\ kg/s$	3.4	3.4
$Q_{IHE}\ kW$	7.7	13.9
$Q_{HEX}\ kW$	60.4	56
$PR_{expansion}$	16.3:1	14.2:1
$VFR_{expansion}$	16:1	12.8:1
$W_{pump}\ kW$	0.7	0.6
$W_{expansion}\ kW$	9.5	9.6
$W_{backpressure+fan\ power}\ kW$	1.4	1.3
$W_{system}\ kW$	6.3	6.6
$\eta_{system\ thermal}\ \%$	10.4	11.8

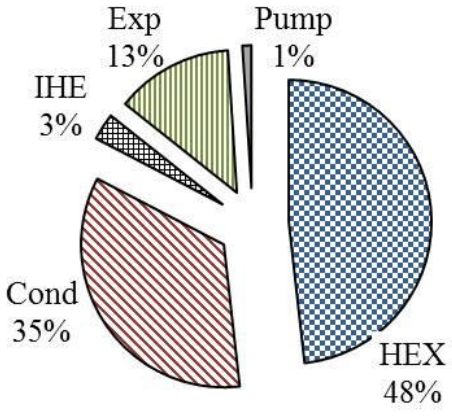

Figure 2 Irreversibility contributions in the fundamental ethanol ORC processes

Fig. 2 presents the component irreversibility contributions in the 52 bar optimal ethanol cycle. It is seen that the HEX made the biggest contribution (48%) followed by the condenser (35%). The high heat transfer irreversibilities were principally due to the temperature differences during near isothermal evaporation/condensation and the high condensing temperature. The expansion (13%) and the pumping (1%) entropy generation rates which were related to the isentropic efficiencies were relatively medium and insignificant, respectively.

The high $T_{boil\ low\ pressure} / T_{boil\ high\ pressure}$ value and heat transfer irreversibility drawbacks are addressed in the published literature by using high VFR expansion machines, more efficient HEXs/condensers and supercritical cycle operation [9, 11, 21]. The supercritical cycle offers lower HEX irreversibilities (avoids near isothermal evaporation) and may allow the exclusion of the IHE (IHE duty decreases with increasing pressure for a fixed temperature). However, Fig. 1b shows that the supercritical ethanol resulted in negligible (3%) system power improvement over the selected 52 bar ethanol cycle. Furthermore, the supercritical cycle required noticeably higher pressure (72 vs. 52 bar) and VFR (23.4:1 vs. 16:1). Although, efficient HEXs/condensers and high VFR expansion machines will be vital in the deployment of ORC systems. These approaches only indirectly address the above drawbacks. Hence, innovative pathways to improve ORC performance and cost-effectiveness remain a major challenge facing the research community.

3 NOVEL FLUID E40

In view of the above understanding, a study was undertaken to identify a single method which for the smallest change to the ethanol ORC with an IHE would translate to a noticeable benefit. The identified path was to formulate a novel organic fluid blend with unique heat transfer and expansion characteristics, while retaining ethanol as a noticeable blend component. Ethanol as a blend constituent was selected since this may allow for the carryover of the developed ethanol components by vehicle manufacturers, original equipment manufacturers, research centres and Tier 1,2 suppliers. Furthermore, ethanol offers a relatively high thermal stability. An evolved screening methodology from previous works was developed and applied to examine over 200 well documented ethanol blends [22-25]. The description of this methodology is beyond the scope of this paper, nonetheless an attempt is made to itemise all the relevant fluid properties.

This section presents the simulation results of a particularly useful blend with varying ethanol concentrations. The resulting different concentration blends were termed based on ethanol percentage by mass, e.g. E80 corresponding to 80% ethanol. (Note: the second blend constituent is undisclosed). Prior to a detailed heat transfer equipment calculation and design, the following was considered for the absolute size comparison. It was assumed that the overall heat transfer coefficient (U, $W/m^2{\bullet}C$) was similar for ethanol and the blends. Therefore, UA (W/°C), i.e. overall heat transfer coefficient multiplied by the heat transfer area (A, m^2), was considered as an indicator for the absolute heat transfer size comparison for HEX, IHE and condenser. Similarly, VFR defined as the ratio between the volumetric flow rates at the expansion outlet to inlet

was considered as an indicator of the absolute size of the expansion machine. The blends were simulated for the same ORC setup (Fig. 1a), but with 20% reduced heat transfer equipment size (i.e. 20% lower UA for HEX, IHE, condenser) and 20% reduced expansion machine size (i.e. 20% lower VFR).

Fig. 3a presents the primary results of interest. Despite the system size reduction, the blends gave nearly equal system power to ethanol. This corresponded to 4.2% of additional engine crankshaft power. The improvements in system thermal efficiency (≈15%) and reduction in the expansion pressure ratio (≈15%) were noticeable. The blend properties were calculated using the Wilson property package [26]. The difference in expansion power was compared against an alternative property package. A low discrepancy of 2% was calculated.

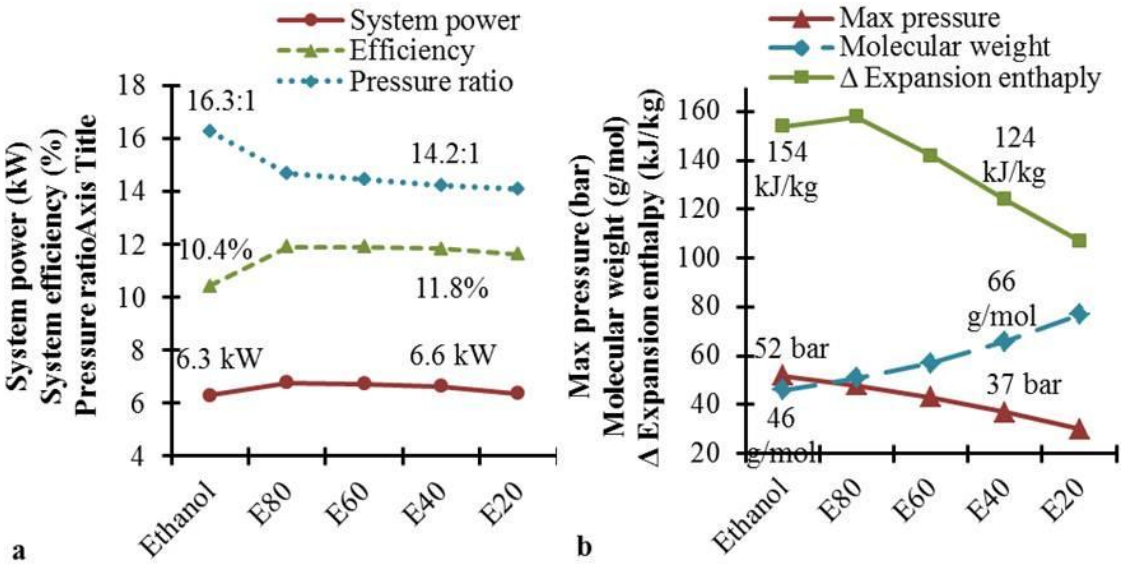

Figure 3 E40 parameters in comparison to ethanol of (a) primary interest and (b) secondary interest

Fig. 3b presents the secondary results of interest. Amongst the blends, E40 was considered as the most appropriate fluid. This was because it offered a suitable trade-off between ethanol concentration, maximum system pressure and molecular weight. Compared to ethanol, E40 required a considerably lower maximum system pressure (37 vs. 52 bar) and offered a much higher molecular weight (66 vs. 46 g/mol).

The lower maximum pressures are advantageous not only for turbines, but also for other positive displacement expanders. This is since under higher pressure operation not only pressure drops and leakages account for a significant portion of performance loss but the machine wear also increases [27]. As a consequence of the higher molecular weight of E40, the expansion enthalpy difference was 30 kJ/kg lower. The lower pressure ratio and higher molecular weight bodes particularly well for single stage turbines as expansion machines. When using a turbine, a 20 g/mol increase in the molecular weight would translate to slightly increased turbine efficiency (from 70% to ≈ 72%) due to design considerations in < 100 kW output capacity [7]. The resulting system power improvements due to this were ignored. Since, a single method to reintroduce the recovered energy into the powertrain has not yet been identified by the HDDE sector.

The use of E40 allows continued examination of both mechanical and electrical methods. Table 2 also summarises the system performance and property values for E40.

To understand the key characteristics of E40, which collectively resulted in nearly equal power to ethanol despite the reduced size, firstly compare the T-S diagrams (Fig. 4a vs. b). The unique heat transfer characteristics of E40 can be summarised as:

- *High ΔT variation during evaporation:* E40 offered a 38°C temperature rise (pt. 3 to pt. 4) compared to the near constant temperature of ethanol. This increases the mean heat addition temperature, and hence, the thermal efficiency. A high ΔT variation during evaporation mirrors the high heat source temperature drop (229°C) and reduces the heat transfer irreversibilities.
- *Higher internal heat recuperation:* The IHE duty for E40 corresponded to 25% of the total heat input, compared to 13% in ethanol. Higher internal heat recuperation decreases the condenser load. This offers lower condensation temperatures for the same cooling air flow rate, resulting in a higher thermal efficiency.
- *Low ΔT variation during condensation:* E40 offered a 14°C temperature rise (pt. 9 to pt. 8) compared to the near constant temperature of ethanol. A low ΔT variation during condensation mirrors the low heat sink temperature rise (15°C) and reduces the heat transfer irreversibilities.

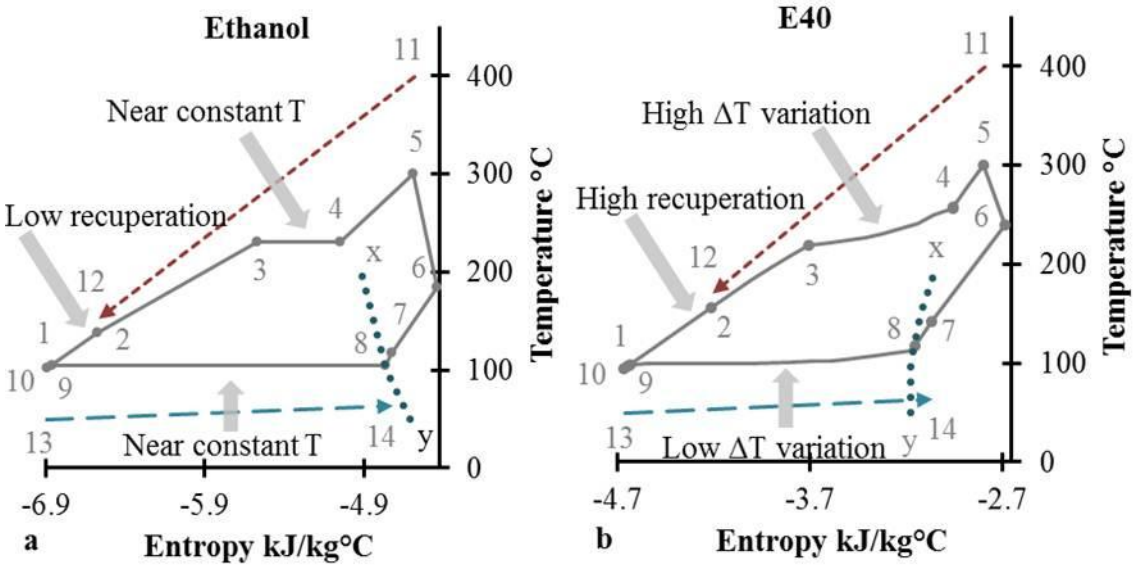

Figure 4 Heat transfer characteristic comparison between (a) ethanol and (b) E40

Secondly, the unique expansion characteristics of E40 can be summarised as:

- *Low* $T_{boil\ low\ pressure} / T_{boil\ high\ pressure}$ *value:* For this illustration consider ethanol and E40 for phase-change at an assumed high and low pressure of 30 and 1 bar and with a fixed duty of 40 kW (Fig. 5). Under these conditions, ethanol gave a value of 0.74. Although E40 offers variable temperature, nonetheless, assuming the average temperature for 10 equal enthalpy intervals during phase-change gave a value of 0.70. This in effect means that under equal high and low system pressures, the maximum and minimum temperature difference for E40 is higher, giving greater area and hence improved efficiency.

- *Suitable for turbines and piston expanders:* E40 is a drying fluid (slope x-y, Fig. 4b), contrary to ethanol. This avoids droplets during expansion when expansion starts at the saturated vapour line, making it suitable for turbines.

Finally, Table 3 presents some key properties for ethanol and E40 for comparison. Both fluids contain carbon, hydrogen and oxygen molecules, and are expected to offer similar boiling points, freezing temperatures, thermal decomposition temperatures, auto-ignition temperatures, NFPA rating and environmental impact [28, 29]. The variation in liquid density, specific heat, thermal conductivity and viscosity is expected to be low (< 20%). Additionally, both fluids have virtually zero electric conductivity and good lubrication properties. Hence, both fluids could be used for cooling the electrical components of the ORC system and lubricating the expansion machine. A preliminary survey result of metals and alloys suited for both ethanol and E40 include aluminium, brass, carbon steel, stainless steel and copper [30-34]. Furthermore, suitable O-ring materials and thermoplastics include ChemRaz, Kalrez, Kel-F, Polyether ether ketone and Polytetrafluoroethylene.

Table 3 Key fluid properties of comparison between ethanol and E40

	Ethanol	E40
Molecular make-up	Carbon Hydrogen Oxygen	Carbon Hydrogen Oxygen
Boiling point °C	77	78
Molecular weight g/mol	46	66
Liquid density kg/m^3	736	795
Specific heat kJ/kg°C	3.31	2.61
Thermal conductivity W/mK	0.15	0.13
Viscosity cP	0.45	0.39
Auto-ignition temperature °C	363	≈390
Decomposition temperature °C	350	≈360
Freezing temperature °C	-114	≈-100
NFPA Health	2	2
NFPA Flammability	3	3
NFPA Reactivity	0	0
Ozone Depletion Potential	0	0
Global warming potential	<20	<20
Electrical conductivity	Nil	Nil
Lubrication properties	Yes	Yes
Cost ($/L for 200L)	36	18
Turbine suitability	+ +	+ + +
Piston expander suitability	+ + + +	+ + + +

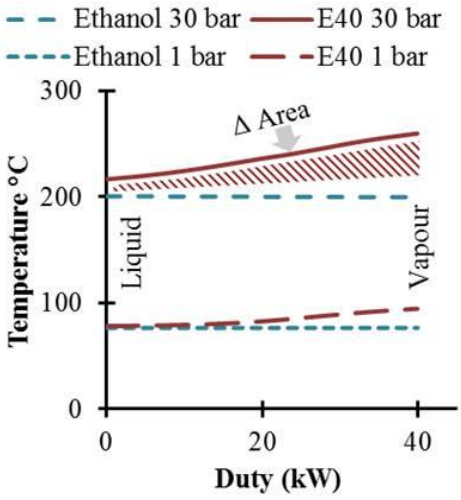

Figure 5 Expansion characteristic comparison between ethanol and E40

4 ECONOMIC ANALYSIS

A detailed economic review and an original cost analysis study conducted for small-scale (5-25 kW), high-production (>1000 units), ORC systems and its associated components resulted in the cost distribution shown in Fig. 6a [35-41]. Three relevant points in the present case were that:

- Only 20% of the total system costs were fixed and non-scalable.
- Scalable fluid expansion, fluid compression and heat transfer costs were closely related to VFR, pressure difference and UA, respectively.
- A similar distribution trend also existed for the size and weight of ORC components (Note: fixed and non-scalable percentage was around 25-30%).

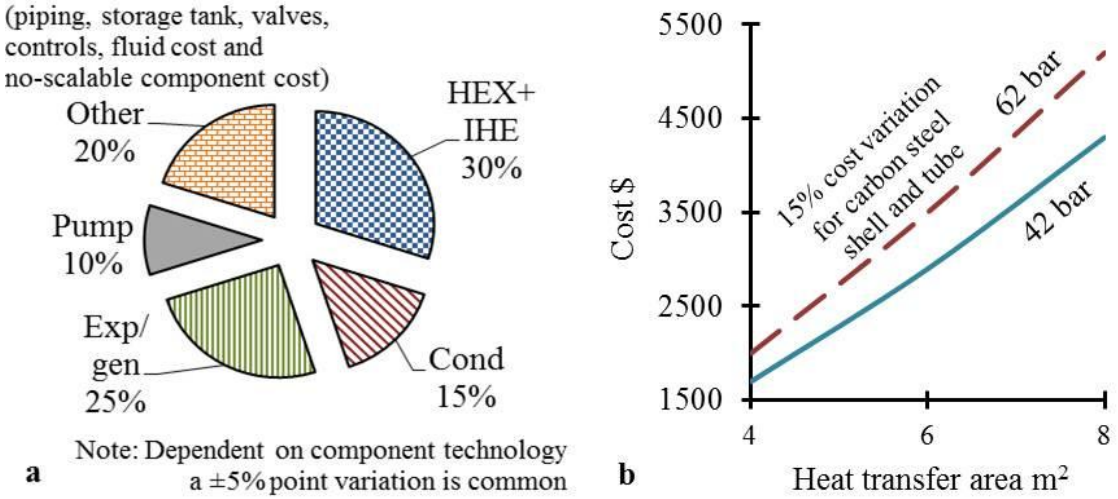

Figure 6 (a) Small scale ORC component cost distribution and (b) Shell and tube heat exchanger pressure vs. cost relationship

To estimate a techno-economical trade-off between ethanol and E40, the following was considered. According to Equation 3, it was assumed that the ratio of Cost/kW of the 52 bar ethanol cycle was 1.

$$Cost / kW = 0.3UA_{HEX+IHE} + 0.15UA_{condenser} + 0.25VFR_{expansion} + 0.1\Delta P_{pump} + 0.2 \ldots (3)$$

Therefore, when considering 20% lower UA and VFR, and 30% lower ΔP for E40, the Cost/kW reduced to 0.83. It is important to emphasise that the additional benefits of the 5% performance improvement (Fig. 3a), expected improvements in turbine efficiency, expected 10% reduction in HEX cost due to lower pressures (Fig. 6b), were all ignored for E40 as a first approximation. A further benefit of E40 not considered was its lower fluid cost. Quotations from two different suppliers indicated that E40 fluid cost was expected to be around half of ethanol (Table 3) [42, 43].

5 CONCLUSIONS

A novel approach has been presented in this paper to facilitate the introduction of ORC systems for HDDE applications. The novelty of the concept developed here consisted of adapting the working fluid make-up to efficiently match the source/sink streams and reduce the cycle pressure difference for a fixed temperature difference. This was achieved by reducing the irreversibilities encountered during the phase-change process

(despite subcritical pressures) and lowering the $T_{boil\ low\ pressure} / T_{boil\ high\ pressure}$ value (despite noticeable ethanol concentration). As a result, for an equal system power to ethanol ORC, the 40% ethanol blend ORC presented the advantages of 15-20% lower volume, weight and cost. This blend offered a higher energy density solution with a favourable system pressure, improving commercialisation potential. The decreased VFR requirement (12.8:1 vs. 16:1) and the increased molecular weight calculated (66 vs. 46 g/mol) allows the possibility of using both single stage radial turbines and piston expanders. This blend is expected to offer the carryover of the currently developed ethanol components, and continued use of both mechanical and electrical power generation methods.

6 REFERENCES

1. US DOE, Advanced Combustion Engine Research and Development, Annual Progress Report. 2011.
2. Baker, H., et al., Review of Low Carbon Technologies for Heavy Goods Vehicles, RD.09/182601.7. 2010.
3. Millikin, M. Daimler Trucks Introduces New Heavy-Duty Engine Platform for North America; DD15 Improves Fuel Economy by 5%. 2007; Available from: www.greencarcongress.com.
4. Kruiswyk, R., J. Fairbanks, and C. Maronde, An Engine System Approach to Exhaust Waste Heat Recovery, in Advanced Combustion Engine Technologies, Annual Progress Report. 2009, 2008.
5. LaGrandeur, J., et al., High-Efficiency Thermoelectric Waste Energy Recovery System for Passenger Vehicle Applications, in Advanced Combustion Engine Research and Development, Annual Progress Report. 2011, 2010, 2009.
6. Stanton, D. The Role of Waste Heat Recovery in Meeting Phase 2 US EPA Greenhouse Gas Regulations. in Diesel Emissions Conference & AdBlue Forum Europe. 2013.
7. Stine, W.B. and M. Geyer, Power Cycles for Electricity Generation, in Power From The Sun. 2001, www.powerfromthesun.net.
8. Crook, A.W., Profiting from Low-grade Heat: Thermodynamic Cycles for Low-temperature Heat Sources. 1994: Institution of Electrical Engineers, ISBN 9780852968352.
9. Seher, D., et al., Waste Heat Recovery for Commercial Vehicles with a Rankine Process in 21st Aachen Colloquium Automobile and Engine Technology, October 8-12, Aachen, Germany. 2012.
10. Halliwell, E., Testing Waste Heat Expanders for New Generation Diesels, in 10th International Conference on Turbochargers and Turbocharging, May 15-16, London, UK. 2012.
11. Edwards, S., et al., Waste Heat Recovery: The Next Challenge for Commercial Vehicle Thermomanagement. SAE Int. J. Commer. Veh., 2012. **5**(1): p. 395-406.
12. Calm, J.M. and G.C. Hourahan, Physical, Safety, and Environmental Data Summary for Current and Alternative Refrigerants, in International Congress of Refrigeration, August 21-26, Prague, Czech Republic. 2011.

13. Zyhowski, G.J. Honeywell Refrigerants Improving the Uptake of Heat Recovery Technologies. 2013; Available from: www.honeywell-orc.com.
14. Teng, H., G. Regner, and C. Cowland, Waste Heat Recovery of Heavy-Duty Diesel Engines by Organic Rankine Cycle Part II: Working Fluids for WHR-ORC. 2007, SAE International, 10.4271/2007-01-0543.
15. Aspen Technology, HYSYS V 7.3. 2011.
16. Johnson, T., Diesel Emission Control in Review. SAE International Journal of Fuels and Lubricants, 2009. **2**(1): p. 1-12.
17. Cloudt, R., F. Willems, and P. van der Heijden, Cost and Fuel Efficient SCR-only Solution for Post-2010 HD Emission Standards. SAE Int. J. Fuels Lubr. 2(1):399-406, 2009.
18. Spurlin M, Gamble C, and Beain A, Defining Thermal Stability, in Process Heating Magazine. 2000.
19. Abdurashidova, A.A., et al., The thermal properties of water-ethanol system in the near-critical and supercritical states. High Temperature, 2007. **45**(2): p. 178-186.
20. Latz, G., S. Andersson, and K. Munch, Comparison of Working Fluids in Both Subcritical and Supercritical Rankine Cycles for Waste-Heat Recovery Systems in Heavy-Duty Vehicles. 2012, SAE International, 10.4271/2012-01-1200.
21. Teng, H. and G. Regner, Improving Fuel Economy for HD Diesel Engines with WHR Rankine Cycle Driven by EGR Cooler Heat Rejection. 2009, SAE International, 10.4271/2009-01-2913.
22. DDBST. Online Dortmund Data Bank Search,. 2014; Available from: ddbonline.ddbst.com.
23. Ponton, J.W. Homogeneous azeotrope databank. Web Tools for Process Engineers. 2007; Available from: eweb.chemeng.ed.ac.uk.
24. Lide, D.R. and H.V. Kehiaian, CRC Handbook of Thermophysical and Thermochemical Data, Volume 1. 1994: Taylor & Francis, ISBN 9780849301971.
25. Horsley, L.H., Azeotropic Data-III, Volume 3. 1973: American Chemical Society, ISBN 9780841205338.
26. Aspen HYSYS V 7.3, Physical Property Methods. 2011.
27. Vincent, L. and Q. Sylvain. Advances in ORC expander design. in International Symposium On Advanced Waste Heat Valorisation Technologies, September 13-14, Kortrijk, Belgium. 2012.
28. NFPA, NFPA 704: Standard System for the Identification of the Hazards of Materials for Emergency Response. 2012.
29. US EPA. Ozone Layer Protection. 2014; Available from: www.epa.gov.
30. eFunda. O-Ring Compatibilities. 2014; Available from: www.efunda.com.
31. Ingersoll Rand, Chemical Compatibility Guide, FORM 8677-P 0508. 2008.
32. Cole-Parmer. Chemical Compatibility Database. 2014; Available from: www.coleparmer.co.uk.
33. allorings.com. O-Ring Fluid Compatibility Guide. 2014; Available from: www.allorings.com.
34. McQuay International. Application Guide AG 31-007: Refrigerants. 2002; Available from: www.daikinmcquay.com.

35. Thekdi, A.C. Waste Heat to Power Economic Tradeoffs and Considerations. in 3rd Annual Waste Heat to Power Workshop, September 25, Houston, USA. 2007.
36. Roos, C.J., An Overview of Industrial Waste Heat Recovery Technologies for Moderate Temperatures Less Than 1000F. 2009, Northwest Clean Heat and Power Application Center. WSUEEP09-26.
37. Dickey, H.K. Low Temperature Geothermal Power Generation with HVAC Hardware. in Geothermal Resource Council, Annual meeting, September 30-October 3, Sparks, USA. 2007.
38. Matches. Process Equipment Cost Estimates. 2014; Available from: www.matche.com.
39. Peters, M., K. Timmerhaus, and R. West, Plant Design and Economics for Chemical Engineers. 2003: McGraw-Hill Education, ISBN 9780072392661.
40. Quoilin, S. and V. Lemort, Technological and Economical Survey of Organic Rankine Cycle Systems, in European Conference on Economics and Management of Energy in Industry, April 14-17, Algarve, Portugal. 2009.
41. Lopes, J., et al., Review of Rankine Cycle Systems Components for Hybrid Engines Waste Heat Recovery. 2012, SAE International, 10.4271/2012-01-1942.
42. Spectrum Chemical Manufacturing Corp. 2014; Available from: www.spectrumchemical.com.
43. ScienceLab. 2014; Available from: www.sciencelab.com.